

# GRAPHENE NANOPATELET REINFORCED THERMALLY INSULATING MICROCHANNEL FOAM

Eric D. Schmid<sup>1</sup>, N. Krishnan P. Veluswamy<sup>1</sup>, Andrew M. Klose<sup>2</sup>,  
James E. Fesmire<sup>3</sup>, and David R. Salem<sup>1</sup>

<sup>1</sup>Composites and Polymer Engineering Laboratory, South Dakota School of Mines & Technology, Rapid City, SD USA

<sup>2</sup>Department of Chemistry, Augustana University, Sioux Falls, SD USA

<sup>3</sup>Cryogenic Test Laboratory, NASA Kennedy Space Center, Cape Canaveral, FL, USA

## ABSTRACT

Graphene nanoplatelets (GNP) have been shown to substantially improve the thermal properties and the mechanical performance in polymer matrix nanocomposite structures. Traditional applications tend to benefit from the simultaneous improvement in both thermal and mechanical multifunctionality, but in the case of polymer nanocomposite insulating foams, the additive/reinforcements must enhance the mechanical properties while also maintaining the low thermal conductivity of the foam. To study the ability of GNP to act as reinforcement for a microchannel epoxy foam structure, loadings of up to 1.00 wt.% GNP were incorporated into the epoxy resin to form the nanocomposite foam matrix. At 0.15 wt.% GNP, nanocomposite foams showed improvements of more than 200% in the microchannel foam specific flexural modulus. These GNP nanocomposite foams also showed no significant change in thermal conductivity as compared to the baseline microchannel polymer foam, thereby demonstrating the ability of GNP microchannel foams as mechanically reinforced thermal insulation. While not yet tested, the addition of the graphene nanoplatelets may potentially provide additional multifunctionality to the foam such as reduced UV/radiation transmittance, improved electrical surface conductivity for diminished static charge buildup, and/or lowering of the coefficient of thermal expansion for enhanced structural stability in extreme environments, making these materials well-suited as high-performance materials supporting applications in next generation space systems.

Keywords: graphene, nanocomposite, microchannel, foam

Corresponding author: Eric Schmid

## 1. INTRODUCTION

Graphene nanomaterials have shown truly exceptional properties and may yet reveal additional unrivaled performance capabilities as new applications are continued to be explored. These applications are driven by the properties of single-layer graphene sheets which have been reported to approach a Young's modulus of approximately 1 TPa, tensile strength of 130 GPa, 97.7% transparency, and electrical and thermal conductivities of over 6000 S/m and 3000 W/m·K, respectively [1,2]. Despite the fact that graphene oxide and reduced graphene oxide are not able to achieve the capabilities of pristine graphene sheets, their use as multi-layer "graphenes" (or graphene nanoplatelets, GNP), has shown success in a variety of nanocomposite applications in recent years. These materials have been used to fabricate aerospace/automotive composites [3,4], EMI shielding [5,6], thermal management materials [7,8], energy storage/conversion devices [8,9],

*Copyright 2021. Used by the Society of the Advancement of Material and Process Engineering with permission.*

*SAMPE neXus Proceedings. Virtual Event, June 29 – July 1, 2021. Society for the Advancement of Material and Process Engineering – North America.*

optical displays [10], electronics/photonic materials [1,11,12], coatings [1], materials with improved flammability resistance [2,12], solar cells [8,11], hydrogen storage materials [4], membranes and separation technologies [9,12], biomedical devices [1,8], and more.

While many applications seek to utilize simultaneous improvements to both the thermal and mechanical properties of the base material, the ability of GNP to provide mechanical reinforcement to thermally insulating foams while maintaining the bulk low thermal conductivity has not been adequately investigated. Specifically, the recent development of microchannel insulating foam structures [13,14] may benefit structurally from the GNP additive, if the thermal conductivity is not significantly increased upon inclusion of the GNP into the polymer matrix structure. While other reports demonstrate increased modulus [2-4,11,15-17], tensile strength [2,4,11,15-17], flexure properties [4,18,19], and fracture toughness [15,16,18-20], the thermal conductivity is also reported to significantly increase [15,21,22]. While these reports are seeking to push the mechanical and thermal boundaries of these material systems, we propose that when used at low loadings, the GNP additives can boost the mechanical properties without compromising the thermal insulation capacity of the microchannel foam.

To study the ability of GNP to act as reinforcement to microchannel foam structures, GNP were dispersed in a diglycidyl ether of bisphenol F epoxy resin and cured with diaminodiphenyl sulfone. The microchannel foams contain hollow microchannel-shaped pores, with the channel fraction, orientation, and diameter being controlled through the use of a thermoplastic templating fiber which is chemically extracted after curing of the thermosetting epoxy resin [13,14]. Furthermore, incorporation of the GNP may not only improve mechanical properties, but also improve radiation/UV shielding [23], increase surface electrical conductivity [2,6,12], and reduce the coefficient of thermal expansion [12]. Microchannel foams fabricated for this study contain microchannel fractions of  $0.65 \pm 0.02$  and densities of  $0.46 \pm 0.03 \text{ g}\cdot\text{cm}^{-3}$ , with microchannel orientations following a [0/90] fabric layup. GNP were added at up to only 1.00% by weight since the increasing resin viscosity ultimately limited the resin transfer by vacuum infusion. GNP nanocomposite foams were characterized with TGA, DSC, three-point flexural testing, and thermal conductivity measurements.

## 2. EXPERIMENTATION

### 2.1 Materials

All materials are commercially available and were used as received. Diglycidyl ether of bisphenol F (DGEBF) resin was purchased from Hexion and provided to Applied Graphene Materials (AGM) to prepare a 5% masterbatch by weight of A-GNP10 graphene nanoplatelets (GNP) in DGEBF by three-roll mill dispersion. The average diameter of these GNP is reported by AGM to be 7-10  $\mu\text{m}$  and only a few nanometers thick. Final resin formulations were comprised of controlled ratios of the GNP masterbatch with additional DGEBF resin, which were then cured with the stoichiometric quantity of 4,4'-diaminodiphenyl sulfone (DDS) curing agent purchased from Huntsman Advanced Materials. After curing of the epoxy resin system, the sacrificial poly(lactic acid) (PLA) microfiber was dissolved using trichloromethane, resulting in epoxy/GNP foam matrix nanocomposites containing the engineered hollow microchannel architectures.

### 2.2 Resin Formulation

Since the GNP are not functionalized for reaction, the stoichiometric ratio (37.28 phr) of DDS was calculated using the reported average equivalent weight of 169 for DGEBF and the

reported DDS reactivity of 63 g/eq. The details of each formulation are summarized in Table 1, with the mass of neat DGEGBF denoted by  $m_{\text{DGEGBF}}$  and the mass of the GNP-DGEGBF 5wt% masterbatch denoted by  $m_{\text{GNP-MB}}$ . The GNP volume percentage was calculated using densities of 1.270 g/cm<sup>3</sup> for the cured DGEGBF/DDS epoxy and 2.2 g/cm<sup>3</sup> for the GNP (as reported in various literature sources [7,18,23]). In this report, all GNP labels are in terms of mass percent relative to the DGEGBF resin.

Table 1. DGEGBF/GNP/DDS formulations

Specimen	Label	$m_{\text{DGEGBF}}$ (g)	$m_{\text{GNP-MB}}$ (g)	$m_{\text{DDS}}$ (g)	wt% GNP <sup>1</sup>	wt% GNP <sup>2</sup>	vol% GNP <sup>2</sup>
DGEGBF/DDS 0.00% GNP	00-GNP	120.0	0.0	44.74	0.000	0.000	0.000
DGEGBF/DDS 0.08% GNP	08-GNP	118.2	1.8	44.70	0.075	0.055	0.032
DGEGBF/DDS 0.15% GNP	15-GNP	116.4	3.6	44.67	0.150	0.109	0.063
DGEGBF/DDS 0.30% GNP	30-GNP	112.8	7.2	44.60	0.300	0.219	0.126
DGEGBF/DDS 0.45% GNP	45-GNP	109.2	10.8	44.53	0.450	0.328	0.190
DGEGBF/DDS 0.60% GNP	60-GNP	105.6	14.4	44.47	0.600	0.438	0.253
DGEGBF/DDS 0.75% GNP	75-GNP	102.0	18.0	44.40	0.750	0.547	0.317
DGEGBF/DDS 0.90% GNP	90-GNP	98.4	21.6	44.33	0.900	0.657	0.380
DGEGBF/DDS 1.00% GNP	100-GNP	96.0	24.0	44.29	1.000	0.730	0.423

(1) relative to DGEGBF resin, (2) relative to the total resin formulation

### 2.3 Specimen Fabrication

Resin formulations were prepared by mixing GNP masterbatch resin and additional DGEGBF resin in the desired quantities according to Table 1. These prepared DGEGBF-GNP resins were pre-heated in an oven for ten minutes at 128°C before the stoichiometric amount of DDS curing agent was added, with the resin then being heated for an additional 80 minutes to completely dissolve the DDS powder, with stirring every ten minutes to promote homogenous mixing and DDS dissolution. This resulting resin was then degassed and VARTM infused at 105°C into the [0/90] microfiber layup as described in previous reports, with the thermoplastic PLA fiber then being sacrificed via post-cure solvolysis to create the desired microchannel foam structures [13,14]. Test specimens were cut from the fabricated panels for chemical, thermal, and physical characterization as described in the next section of this report, with primary focus being on the mechanical (three-point flexure) properties and cryogenic thermal conductivity of the GNP-containing microchannel foams.

### 2.4 Characterization Methods

Prior to part fabrication, selected DGEGBF/GNP resin ratios were characterized by FTIR and rheological methods to investigate effects of GNP on the uncured resin properties. ATR-FTIR spectra of the constituent materials were obtained using a model Nicolet iS50 Thermo-Scientific spectrometer, with 32 scans collected for each sample with a resolution of 4 cm<sup>-1</sup> from 400 to 4000 cm<sup>-1</sup>. Resin viscosity was measured using a temperature-controlled DV-III Ultra Brookfield rheometer with SC4-27 spindles.

After resin infusion, curing, and microfiber dissolution, the DGEGBF/GNP/DDS microchannel specimens were examined with both TGA and DSC to determine any changes in the material thermal stability. TGA data were collected under a nitrogen environment with the

Shimadzu TGA-50 at a rate of 10°C/min. DSC was performed using a Shimadzu DSC-60 Plus Differential Scanning Calorimeter with aluminum pans at a rate of 10°C/min under dry air.

The mechanical properties of the microchannel nanocomposite foam specimens were measured by means of three-point flexure testing (according to ASTM D790 Procedure A - Standard Test Method for Flexural Properties of Unreinforced and Reinforced Plastics and Electrical Insulating Materials) with the span set to 50.8 mm and crosshead testing rates calculated according to the standard method. Typical specimens were approximately 64 mm x 12 mm x 3 mm. Flexural moduli were calculated using the stress-strain curves and flexural strengths were calculated at the specimen break points.

Thermal conductivity testing was performed at NASA Kennedy Space Center's Cryogenics Test Laboratory (CTL) and Cryotek, LLC utilizing a novel comparative flat-plate liquid nitrogen (LN2) boiloff calorimeter, referred to as the Macroflash, in accordance with ASTM C1774, Annex A4 [24]. Round disk specimens 76.2 mm in diameter were stacked in pairs to form test articles 6.35 mm tall, with test data being collected under steady state LN2 boiloff conditions. Thermal grease and 5 psi compression were applied to minimize insulative effects at the interfacial boundary, with data being produced in terms of the effective thermal conductivity ( $k_e$ ) using boundary temperatures of 78K and 293K.

### 3. RESULTS

#### 3.1 Resin Properties

FTIR spectra of the neat DGEBF resin and the 5wt.%GNP masterbatch in DGEBF are compared in Figure 1. While the neat DGEBF resin is clear and colorless, addition of GNP turns the resin opaque black (as shown in the inset image of glass vials in Figure 1). However, since the GNP are non-functionalized the FTIR spectra remains unchanged from that of the representative uncured DGEBF spectra, with the epoxide vibration at 910-917  $\text{cm}^{-1}$  indicative of the uncured epoxy resin system [25]. At the low GNP loadings used in this study, the GNP is not anticipated to restrict the epoxide curing mechanism in any way. This will be further discussed in the FTIR analysis of the foam characterization section.

The viscosities of the uncured DGEBF/GNP resins were measured to study limits in the vacuum infusion process. Since well-dispersed nanomaterials are known to increase resin viscosity, it was anticipated there would be an upper limit to the percentage of GNP additive able to be infused using the vacuum assisted resin transfer method. Typically, a 500 cP or less rule-of-thumb is applied for standard composites manufacturing in order to achieve acceptable infusion rates. In this study, the epoxy resin viscosity was observed to increase from approximately 6000 cP (neat DGEBF) to 150,000 cP for 5wt.% GNP dispersed in DGEBF. While 6000 cP is above the desired infusion rule-of-thumb, heating the resin can sufficiently lower the viscosity to facilitate infusion (as long as the increased temperature does not significantly accelerate the curing mechanism of the epoxy formulation). We demonstrate this approach by performing the infusion at 105°C rather than at room temperature. While in-depth temperature-viscosity studies are beyond the scope of this analysis, we have experimentally determined the viscosity limit to be met at approximately 1.0% GNP by weight, at which the resin was only able to be vacuum infused into the microfiber layup to no more than a couple of centimeters even at elevated temperatures.

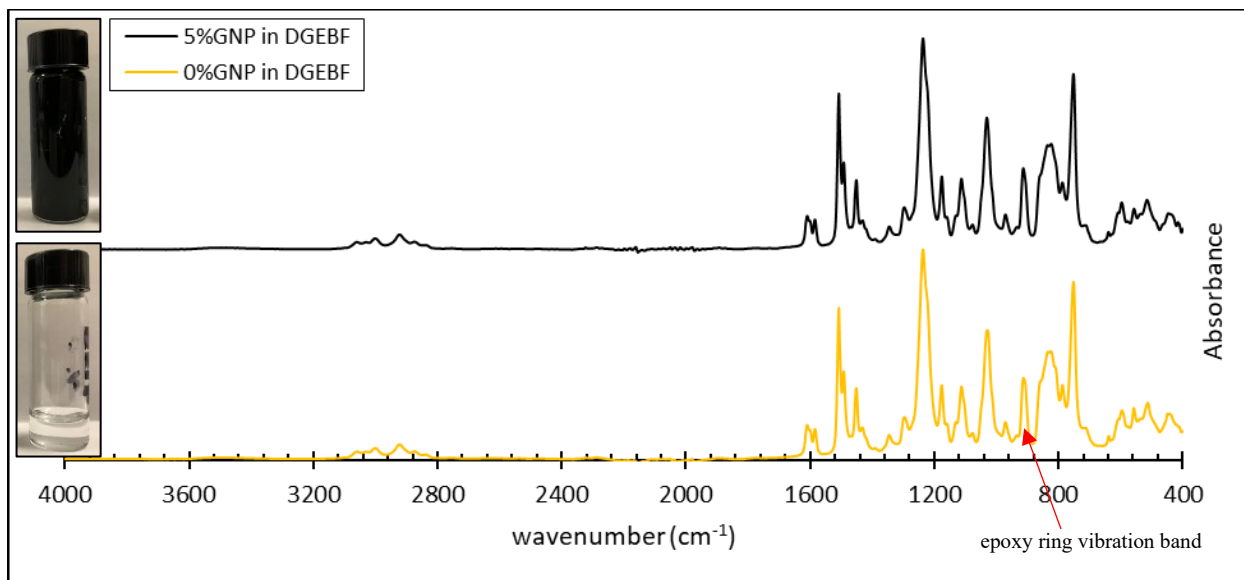


Figure 1. FTIR spectrum of uncured neat DGEBF (bottom) compared to DGEBF with 5wt% GNP (top).

### 3.2 Characterization of Epoxy/GNP Microchannel Foams

After curing and dissolution of the microfiber template, the resulting epoxy/GNP microchannel foams were characterized using chemical and thermal methods. Additionally, the thermal conductivities and mechanical properties of these epoxy/GNP microchannel foams were evaluated for comparison to the performance of epoxy microchannel foams not containing GNP additives.

FTIR of the cured epoxy microchannel foams were performed to ensure full epoxy curing. As shown in Figure 2 the epoxide band ( $910\text{-}917\text{ cm}^{-1}$ ) in the DGEBF resin prior to cure disappears and the  $1103\text{ cm}^{-1}$  band appears in the microchannel foams after the cure, implying the GNP additive did not hinder the epoxide curing process. Since these FTIR peaks representing the uncured resin constituents have been fully consumed, this indicates the microchannel foam GNP nanocomposites have reached full cure.

Polymer thermal stability is often increased via addition of nanomaterials, which restrict molecular mobility of the polymer chains and hinder molecular diffusion. The thermal stability of the GNP nanocomposite foams was assessed using both DSC to determine changes in the glass transition temperature ( $T_g$ ) and TGA to identify shifts in degradation onset temperature ( $T_{5\%}$ ), 50% residual mass temperature ( $T_{50\%}$ ) and char yield ( $m_R$ ) for comparison to the uncured resin system. The  $T_g$  of the foams were determined to be essentially unaffected by the GNP additive (Table 2), with an average  $T_g$  across all specimens of  $174.3 \pm 0.6^\circ\text{C}$ . While some studies have reported on the ability of graphene to increase the glass transition temperature by approximately  $10\text{-}20^\circ\text{C}$  at low GNP loadings [18, 26], others have reported inconsistent  $T_g$  results due to reduced dispersion or poor GNP-resin interfacing during the curing process [9,12]. Neither an improvement nor a loss in performance was noted in this study, perhaps indicating the GNPs are adequately dispersed but suffer from poor interfacing with the epoxy resin, which may result in an increase in free volume and offset any potential gains in thermal stability. This may also explain why the TGA data, summarized in Table 2, reveals no significant improvements to the  $T_{5\%}$  ( $292 \pm 5^\circ\text{C}$ ) and  $T_{50\%}$  ( $452 \pm 4^\circ\text{C}$ ) regardless of the GNP content, with a final average residual mass  $m_R$  of only 0.7%. While no substantial improvements to thermal stability have been noted, the fact that there is no reduction

in thermal stability relative to the neat epoxy materials may indicate the GNP have maintained adequate dispersion during the resin cure, thus forming the desired nanocomposite structure within the foam matrix.

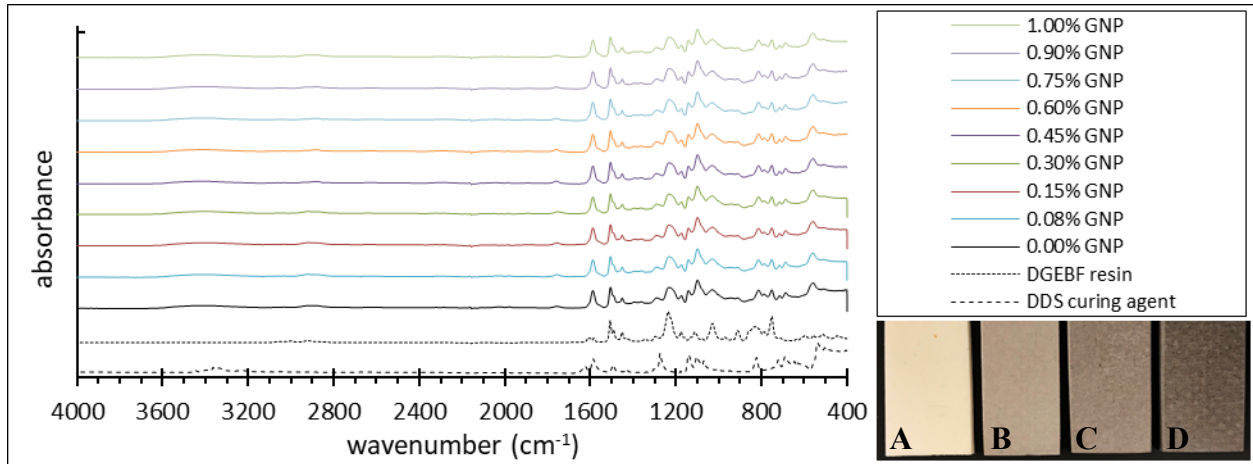


Figure 2. FTIR spectra of cured microchannel epoxy foams containing GNP compared to uncured resin components. Inset image shows selected microchannel epoxy foams with increasing amounts of GNP from A) 0.00% GNP, B) 0.30% GNP, C), 0.60% GNP, to D) 1.00% GNP.

Table 2. Thermal properties of GNP reinforced microchannel foams

Label	T <sub>g</sub> (°C)	T <sub>5%</sub> (°C)	T <sub>50%</sub> (°C)	m <sub>R</sub> (%)
00-GNP	174.3	285.7	444.0	0.5
08-GNP	174.1	296.3	450.6	0.6
15-GNP	173.6	291.6	454.1	0.3
30-GNP	173.6	289.3	449.7	0.9
45-GNP	174.4	291.6	451.9	1.0
60-GNP	174.4	292.8	454.9	1.2
75-GNP	174.3	291.9	458.0	1.0
90-GNP	174.6	300.6	453.8	0.3
100-GNP	175.7	286.3	446.5	0.7

As discussed in the introduction, most GNP reinforcement applications simultaneously achieve enhancement of both the mechanical properties and thermal conductivity. However, GNP may provide advantageous multifunctional performance for insulative foams as well, as long as the total GNP percentage remains below the percolation threshold of the foam matrix to prevent the formation of interconnected thermally conductive pathways.

GNP nanocomposite microchannel foam specimens were prepared for thermal conductivity testing, with final average microchannel fractions of  $0.65 \pm 0.02$  and densities of  $0.46 \pm 0.03 \text{ g}\cdot\text{cm}^{-3}$  across the tested specimens. After measuring the thermal conductivity using the Macroflash liquid nitrogen boiloff technique, the relative thermal conductivity was calculated and plotted as a function of the relative density (shown in Figure 3). This data confirms no significant increase in thermal conductivity over the GNP range tested, despite the reported high thermal conductivity values for GNP additives. While 0.75% GNP is still a relatively small amount of additive by most standards, a simple rule-of-mixtures calculation would expect the thermal conductivity of these foams to increase from approximately  $0.2 \text{ W/m}\cdot\text{K}$  to more than  $30 \text{ W/m}\cdot\text{K}$ . Instead, the data shown in Figure 3 confirms the thermal conductivity of these reinforced microchannel foams to remain within the normal deviation of the baseline conductivity data (with

$\pm 5\%$  from the model being shown by the dashed lines). This aligns with our previous work using reinforcing polymer-ceramic hybrid additives [27], in which the hollow microchannel structure creates a dominant insulating effect which masks any minor contributions to the solid-state thermal conductivity from the incorporated additives. Similarly, while the GNP are fully dispersed within the foam matrix filaments and struts, using a low total percentage of GNP ensures the percolation threshold is not reached, thus allowing the otherwise conductive nano-additive to serve primarily as a mechanical reinforcement while still retaining the bulk insulative performance of the polymer-based foam.

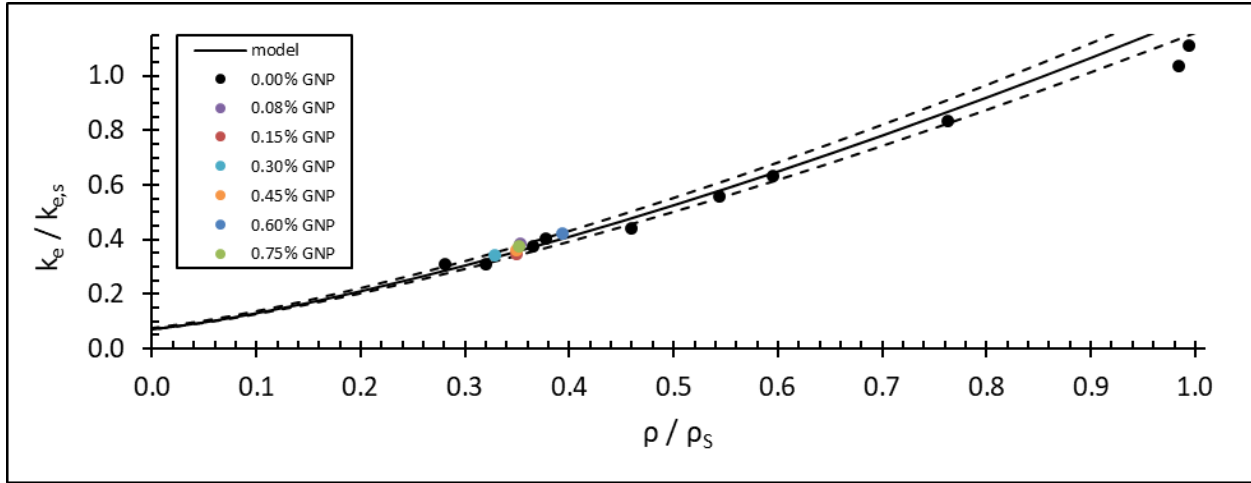


Figure 3. Thermal conductivity of microchannel epoxy foam specimens containing up to 0.75% GNP.

To investigate the opportunity for using GNP as a reinforcement material without increasing thermal conductivity, a series of GNP reinforced microchannel foams were fabricated to contain GNP fractions ranging from 0.075% to 1.00% in the epoxy foam matrix structure, with samples having an average microchannel fraction of  $0.64 \pm 0.01$  and densities of  $0.46 \pm 0.02 \text{ g} \cdot \text{cm}^{-3}$  across the mechanical testing specimens.

The effect of GNP on the microchannel flexural strength and stiffness is shown in Figures 4 and 5. Figure 4 shows the GNP reinforced microchannel foam three-point flexure data alongside that of the three-point flexure strength ( $\sigma_F$ ) and stiffness ( $E_F$ ) baseline data sets collected in our previous studies for non-reinforced microchannel epoxy foams [13]. This data is plotted as a function of relative density, in which the density of each foam is normalized to the rule-of-mixtures density expected based on the constituent makeup of each specimen. Figure 5 shows the specific strength and specific stiffness of the GNP reinforced microchannel foams as a function of the GNP loading. The combination of these data sets helps elucidate the true impact of the GNP on the flexural strength and stiffness of the microchannel foam materials. As shown in Figure 4A, the addition of up to 1.00% GNP to the matrix recipe does not provide any substantial improvement to microchannel foam strength. This aligns with other reports which have described the great challenge of increasing material strength with non-fiber additives [28]. However, Figure 4B reveals the flexural moduli of the microchannel foams to be significantly enhanced using the GNP additive, even at very low loading levels. From this data, it is observed that the foam modulus is improved at all GNP loadings up to 0.75% GNP, upon which higher levels of GNP result in a reduction of material stiffness towards that of the baseline epoxy foam. We believe this reduction may be due to aggregation of the GNP at higher loadings which results in reduced dispersion, higher localized stress concentrations, and a corresponding return to baseline foam material

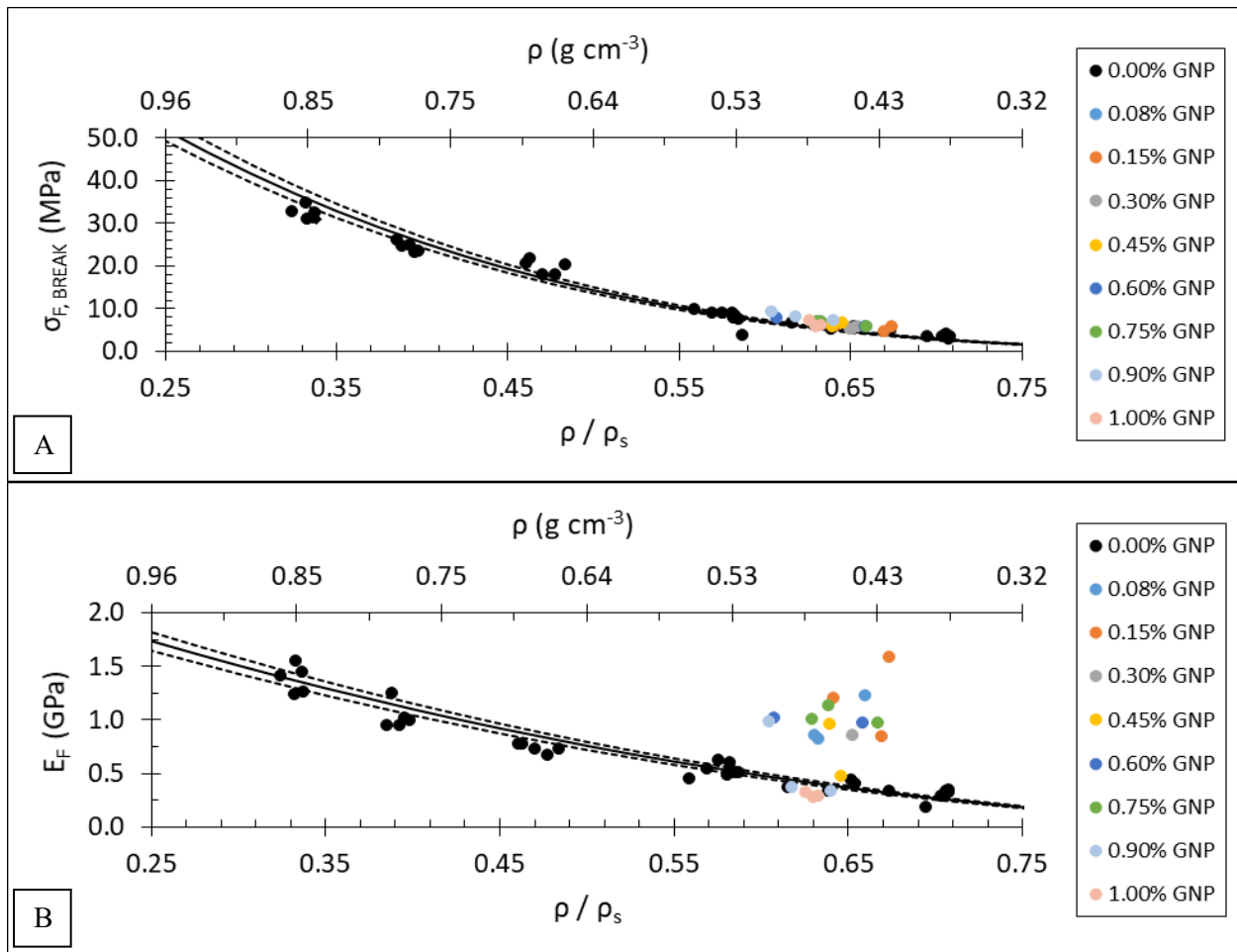


Figure 4. Effect of GNP additive by weight on microchannel epoxy foam A) strength and B) stiffness.

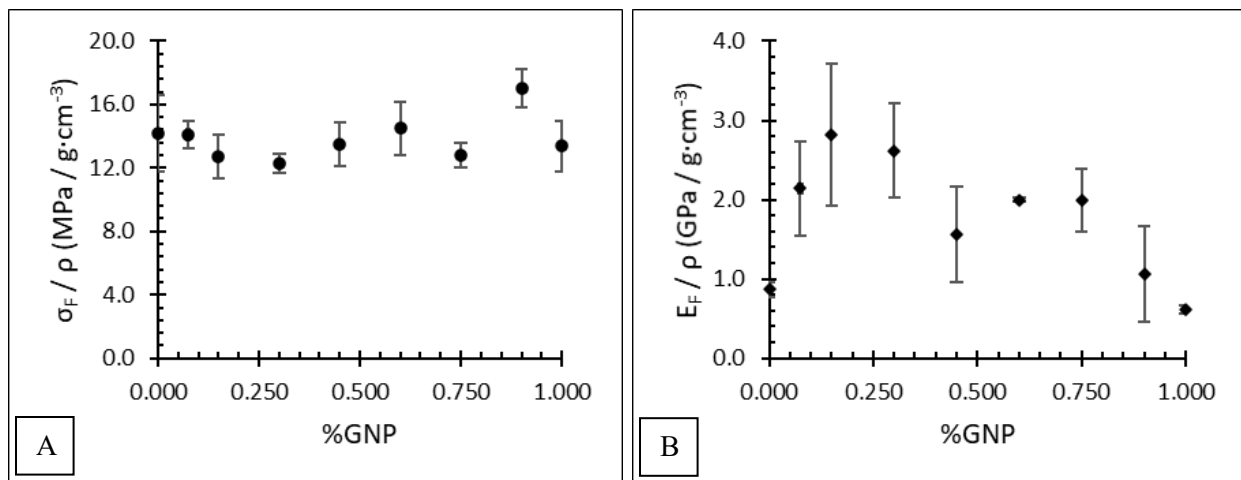


Figure 5. Specific A) strength and B) stiffness of GNP reinforced microchannel foams as a function of GNP loading.

stiffness. Additionally, poor interfacial adhesion at higher GNP loadings may also increase local stress points, resulting in interfacial debonding at lower applied forces as compared to specimens with lower GNP fractions. These two mechanisms must be overcome to ensure high-quality

nanocomposite structures, and it seems in this case that loadings of less than 0.75% GNP demonstrate suitable dispersion and interfacial adhesion with the epoxy resin.

The specific strength and stiffness were calculated to account for the relative differences in each specimen's density and are plotted as a function of GNP loading in Figure 5. Combined with the data shown in Figure 4, we see that the increase in specific modulus peaks at GNP loading of 0.15%, resulting in an increase of more than 226% relative to the non-reinforced microchannel foam. The specific strength remains essentially constant from 0.0 to 1.0% GNP. It is possible the poor GNP-epoxy interfacing is limiting the nanocomposite strength (which may also be reflected in the TGA data). However, there is still clearly a significant improvement to the flexural modulus achieved at very low loadings of GNP, making these nanocomposite materials not only economically suitable for reinforced thermal insulation, but also for other applications which may take advantage of the anisotropic microchannel architecture.

#### **4. CONCLUSIONS**

A series of DGEBF/DDS epoxy resin systems were formulated to contain increasing fractions of graphene nanoplatelets (GNP) in efforts to achieve nano-reinforced microchannel foams with enhanced multifunctionality while simultaneously retaining their excellent thermal insulation capabilities. Challenges associated with an increased infusion viscosity ultimately limited the total fraction of GNP utilized in the VARTM fabricated test articles to no more than 1.00% GNP by weight, but while infusion rule-of-thumb suggests viscosities must be 500 cP or less, increasing the infusion processing temperature to 105 °C resulted in a viscosity sufficiently low to allow for appreciable vacuum assisted resin infusion rates. Despite this manufacturing challenge, microchannel foams were fabricated containing from 0.075% to 1.0% GNP for thermal and mechanical characterization. Compared to the neat epoxy microchannel foam baseline properties, GNP additive up to 0.75% did not significantly increase the thermal conductivity of the specimens. However, the addition of up to 0.75% GNP did enhance the three-point flexural moduli of these foam structures, with specific moduli values showing the most improvement (of more than 226%) at GNP weight fractions of only 0.15%. This combination of improved mechanical performance and retained very low thermal conductivities is unique among the literature, as most applications seek to substantially improve both thermal and mechanical properties simultaneously. Furthermore, in addition to the economic benefits of utilizing a very low level of GNP additive, other advantageous multifunctionalities are also anticipated due to the reported wide variety of beneficial GNP properties, which include but are certainly not limited to improved UV/radiation shielding capabilities, enhanced static surface charge dissipation, and lower coefficients of thermal expansion. These properties make the GNP reinforced microchannel foams particularly promising as lightweight material solutions for engineered structures and thermal insulation systems for future space missions.

#### **5. ACKNOWLEDGEMENTS**

This work was performed at the Composites and Polymer Engineering (CAPE) Laboratory at the South Dakota School of Mines & Technology (SDSMT), the Cryogenics Test Laboratory (CTL) at NASA Kennedy Space Center, and Cryotek LLC. Funding was provided by NASA EPSCoR grant #NNX12AB17G and the South Dakota Space Grant Consortium Research Stipend Program. Personnel support from the CAPE Laboratory, NASA CTL, Cryotek LLC, and the

Composite and Nanocomposite Manufacturing (CNAM) Center at SDSMT are also greatly appreciated.

## 6. REFERENCES

1. Yi M, Shen Z. A review on mechanical exfoliation for scalable production of graphene. *J Mater Chem A* 3 (2015): 11700-11715
2. Smith AT, LaChance AM, Zeng S, Liu B, Sun L. Synthesis, properties, and applications of graphene oxide/reduced graphene oxide and their nanocomposites. *Nano Mater Sci* 1 (2019): 31-47
3. Yadav SK, Cho JW. Functionalized graphene nanoplatelets for enhanced mechanical and thermal properties of polyurethane nanocomposites. *Appl Surf Sci* 266 (2013): 360-367
4. Papageorgiou DG, Kinloch IA, Young RJ. Mechanical properties of graphene and graphene-based nanocomposites. *Prog Mater Sci* 90 (2017): 75-127
5. Liang J, Wang Y, Huang Y, Ma Y, Liu Z, Cai J, Zhang C, Gao H, Chen Y. Electromagnetic interference shielding of graphene/epoxy composites. *Carbon* 47 (2009): 922-925
6. Monti M, Rallini M, Puglia D, Peponi L, Torre L, Kenny J. Morphology and electrical properties of graphene-epoxy nanocomposites obtained by different solvent assisted processing methods. *Compos Part A* 46 (2013): 166-172
7. Abbasi H, Antunes M, Velasco JI. Effects of graphene nanoplatelets and cellular structure on the thermal conductivity of polysulfone nanocomposite foams. *Polymers* 12 (2020): 25
8. Sang M, Shin J, Kim K, Yu KJ. Review – Electronic and thermal properties of graphene and recent advances in graphene based electronics applications. *Nanomaterials* 9 (2019): 374
9. Guan LZ, Zhao L, Wan YJ, Tang LC. Three-dimensional graphene-based polymer nanocomposites: preparation, properties and applications. *Nanoscale* 10 (2018):14788-14811
10. Li Y, Chopra N. Progress in large-scale production of graphene. Part 1: chemical methods. *JOM* 67 (2015): 34-43
11. Paton KR, et. al. Scalable production of large quantities of defect-free few-layer graphene by shear exfoliation in liquids. *Nat Mater* 13 (2014): 624-630
12. Potts JR, Dreyer DR, Bielawski CW, Ruoff RS. Graphene-based polymer nanocomposites. *Polym* 52 (2011): 5-25
13. Schmid E, Robinson M, Cross W, Salem D. Tensile, flexure, and compression properties of anisotropic microchannel epoxy foams. *J Appl Polym Sci* 136 (2019): 47945
14. Schmid E, Salem D. Fabrication technique and thermal insulation properties of micro- and nano-channeled polymer composites, *Acta Astronaut* 116 (2015): 68-73
15. Wang F, Drzal LT, Qin Y, Huang Z. Mechanical properties and thermal conductivity of graphene nanoplatelet/epoxy composites. *J Mater Sci* 50 (2015): 1082-1093
16. Raflee M, Raflee J, Wang Z, Song H, Yu ZZ, Koratkar N. Enhanced mechanical properties of nanocomposites at low graphene content. *ACS Nano* 12 (2009): 3884-3890
17. Xu Z, Gao C. In situ polymerization approach to graphene-reinforced nylon-6 composites. *Macromol* 43 (2010): 6716-6723

18. Tang LC, Wan YJ, Yan D, Pei YB, Zhao L, Li YB, Wu LB, Jiang JX, Lai GQ. The effect of graphene dispersion on the mechanical properties of graphene/epoxy composites. *Carbon* 60 (2013): 16-27
19. Wang PN, Hsieh TH, Chiang CL, Shen MY. Synergetic effects of mechanical properties on graphene nanoplatelet and multiwalled carbon nanotube hybrids reinforced epoxy/carbon fiber composites. *J Nanomater* (2015): 1-9
20. Chatterjee S, Nuesch FA, Chu BTT. Comparing carbon nanotubes and graphene nanoplatelets as reinforcements in polyamide 12 composites. *Nanotech* 22 (2011): 275714
21. Ganguli S, Roy AK, Anderson DP. Improved thermal conductivity for chemically functionalized exfoliated graphite/epoxy composites. *Carbon* 46 (2008): 806-817
22. Guo Y, Xu G, Yang X, Ruan K, Ma T, Zhang Q, Gu J, Wu Y, Liu H, Guo Z. Significantly enhanced and precisely modeled thermal conductivity in polyimide nanocomposites with chemically modified graphene via in situ polymerization and electrospinning-hot press technology. *J Mater Chem C* 6 (2018): 3004-3015
23. Gedlar G, Antunes M, Borca-Tasciuc T, Velasco JI, Ozisik R. Effects of graphene concentration, relative density and cellular morphology on the thermal conductivity of polycarbonate-graphene nanocomposite foams. *Eur Polym J* 75 (2016): 190-199
24. Fesmire J, Bateman C, Thomas J. Macroflash apparatus and boiloff calorimetry method for the measurement of heat transmission through materials. International Cryogenic Materials Conference, Hartford, CT, 21-25 July 2019 (in publication).
25. Ramirez C, Rico M, Torres A, Barral L, Lopez J, Monero B. Epoxy/POSS organic-inorganic hybrids: ATR-FTIR and DSC studies. *Eur Polym J* 44 (2008): 3035-3045
26. Yan D, Xu L, Chen C, Tang J, Ji X, Li Z. Enhanced mechanical and thermal properties of rigid polyurethane foam composites containing graphene nanosheets and carbon nanotubes. *Polym Int* 61 (2012): 1107-1114
27. Rashid E, Ariffin K, Kooi C, Akil H. Preparation and properties of POSS/epoxy composites for electronic packaging applications. *Mater Des* 30 (2009): 1-8
28. Schmid ED, Veluswamy NKP, Salem DR. Mechanical and thermal properties of microchannel insulating foams comprising a multifunctional epoxy/polyhedral oligomeric silsesquioxane nanocomposite. *Polym Comp* 41 (2020): 5030-5042